International Journal of Nanomedicine

Dovepress
open access to scientific and medical research

Open Access Full Text Article

ORIGINAL RESEARCH

Lipid-polymer hybrid nanoparticles for controlled delivery of hydrophilic and lipophilic doxorubicin for breast cancer therapy

This article was published in the following Dove Press journal:
International Journal of Nanomedicine

Nayab Tahir[1–3]
Asadullah Madni[2]
Alexandra Correia[3]
Mubashar Rehman[4]
Vimalkumar Balasubramanian[3]
Muhammad Muzamil Khan[2]
Hélder A Santos[3,5]

[1]College of Pharmacy, University of Sargodha, Sargodha, Pakistan; [2]Department of Pharmacy, The Islamia University of Bahawalpur, Bahawalpur 63100, Pakistan; [3]Drug Research Program, Division of Pharmaceutical Chemistry and Technology, Faculty of Pharmacy, University of Helsinki, Helsinki FI-00014, Finland; [4]Department of Pharmacy, The University of central Pujnab, Lahore, Pakistan; [5]Helsinki Institute of Life Science (HiLIFE), University of Helsinki, Helsinki FI-00014, Finland

Background: Lipid polymer hybrid nanoparticles (LPHNPs) for the controlled delivery of hydrophilic doxorubicin hydrochloride (DOX.HCl) and lipophilic DOX base have been fabricated by the single step modified nanoprecipitation method.

Materials and methods: Poly (D, L-lactide-co-glicolide) (PLGA), lecithin, and 1,2-distearoyl-Sn-glycero-3-phosphoethanolamine-N-[methoxy (polyethylene glycol)-2000 (DSPE-PEG 2000) were selected as structural components.

Results: The mean particle size was 173–208 nm, with an encapsulation efficiency of 17.8 ±1.9 to 43.8±4.4% and 40.3±0.6 to 59. 8±1.4% for DOX.HCl and DOX base, respectively. The drug release profile was in the range 33–57% in 24 hours and followed the Higuchi model (R^2=0.9867–0.9450) and Fickian diffusion (n<0.5). However, the release of DOX base was slower than DOX.HCl. The in vitro cytotoxicity studies and confocal imaging showed safety, good biocompatibility, and a higher degree of particle internalization. The higher internalization of DOX base was attributed to higher permeability of lipophilic component and better hydrophobic interaction of particles with cell membranes. Compared to the free DOX, the DOX.HCl and DOX base loaded LPHNPs showed higher antiproliferation effects in MDA-MB231 and PC3 cells.

Conclusion: Therefore, LPHNPs have provided a potential drug delivery strategy for safe, controlled delivery of both hydrophilic and lipophilic form of DOX in cancer cells.

Keywords: lipid polymer hybrid, doxorubicin, breast cancer, nanotechnology, drug delivery

Introduction

Cancer is ranked among the most highly prevalent diseases and is the second leading cause of mortality and morbidity globally.[1] According to the World Health Organization (WHO), prostate cancer is listed as the most commonly occurring cancer among males (ca. 25% of all the newly diagnosed patients) and breast cancer among females (more than 25% of total cases).[2] Use of different chemotherapeutic agents has been employed as the most efficient approach for the treatment of the cancer. Currently, doxorubicin (DOX), etoposide, docetaxel, and cisplatin are considered most effective chemotherapeutic agents.[3] However, the delivery of these chemotherapeutic agents might be associated with multi-faceted challenges, such as a lack of specificity to retain the therapeutic agent in the cancer environment, low solubility in the aqueous media, rapid elimination, and non-specific distribution, demanding larger dose administration, which leads to dose-related toxicities.[4,5]

Correspondence: Asadullah Madni
Department of Pharmacy, The Islamia University of Bahawalpur, Bahawalpur 63100, Pakistan
Tel +9 262 925 5243
Email asadpharmacist@hotmail.com

Hélder A Santos
Drug Research Program, Division of Pharmaceutical Chemistry and Technology, Faculty of Pharmacy, University of Helsinki, Helsinki FI-00014, Finland
Tel +35 829 415 9661
Email helder.santos@helsinki.fi

submit your manuscript | www.dovepress.com
DovePress
http://doi.org/10.2147/IJN.S209325

Nanotechnology presents an advanced platform for the treatment of cancer by developing novel nanocarriers systems for the administration of chemotherapeutic agents, ranging from the small hydrophilic and lyophilic molecules to large peptides and proteins.[6] In the last few decades, various nano-sized drug delivery systems (DDS) have been designed, fabricated, and approved for clinical use, while a large number of DDS are still under clinical trials for the diagnostic and therapeutic applications.[7] Polymeric DDS and lipid based nanocarriers have been listed as the most important systems. Liposomal carriers offer advantages in terms of better compatibility, superior pharmacokinetic characteristics, longer retention time, and easy surface modulation. Moreover, the polymeric carriers offer prolonged and controlled drug release from the system and excellent stability profiles. Despite all of these properties, both liposomes and polymeric carrier systems have limitations in terms of drug stability, drug leakage, low loading capacity, and compatibility.[8]

Recently, the integration of these systems (liposomes and polymeric nanoparticles, NPs) provide a novel domain of DDS, termed as the lipid polymer hybrid nanoparticles (LPHNPs), that hold promising applications in the diagnostic imaging and treatment of different carcinomas, as shown in Figure 1.[9] In contrast to other carriers, the LPHNPs offer some unique features, including the diversity in structural components, higher encapsulation, controlled drug release, biocompatibility, improved stability profile, enhanced permeability, and cellular uptake.[10,11] These particles also have the capacity to encapsulate the hydrophilic and hydrophobic therapeutic moieties.

DOX is an antineoplastic agent of non-selective class I anthracycline antibiotics class that are regarded as the most effective anticancer drugs.[12] It has been clinically employed alone or in combination for treating various carcinomas.[13] Despite of its potential benefits, DOX also have dose dependent cardiac toxicities, such as congestive heart failure and chronic cardiomyopathy.[14] Different studies have reported superior efficacy of nano-encapsulated hydrophilic DOX.HCl and lipophilic DOX. However, limited studies were performed previously to study the difference in the chemical form and the hydrophobicity on the antitumor activity of DOX.

In this study, we developed DOX.HCl and DOX base encapsulated LPHNPs by using the self-assembling modified nanoprecipitation method. The main aim of the study was to compare the physicochemical and therapeutic properties of the DOX.HCl and DOX base that provide the sightful information about the co loading of hydrophilic and lipophilic drugs in the LPHNPs for better drug therapy. Poly (D, L-lactide-co-glicolide) (PLGA) was employed as an inner core material, owing to its biodegradable and biocompatible nature. Likewise, the mixture of lecithin and 1,2-distearoyl-Sn-glycero-3-phosphoethanolamine-N-[methoxy (polyethylene glycol)-2000 (DSPE-PEG 2000) was used as lipid. LPHNPs were characterized for various physicochemical, compatibility, and solid state properties. In addition to physicochemical characterization, the DOX.HCl and DOX-base-loaded LPHNPs were fabricated with different drug-to-polymer ratios compared to the drug loading, entrapment, and drug release behavior. The in vitro cytotoxicity, antiproliferative activity, and cell uptake studies were performed to simulate the in vivo fate and activity of these LPHNPs in various cancerous cells to determine any difference in the activity of DOX.HCl and DOX base loaded in the LPHNPs.

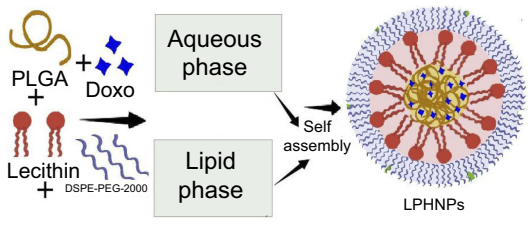

Figure 1 Schematic diagram of the LPHNPs.
Abbreviations: Doxo, Doxorubicin; DSPE-PEG 2000, 1,2-distearoyl-Sn-glycero-3-phosphoethanolamine-N-[methoxy (polyethylene glycol)]-2000; LPHNPs, lipid polymer hybrid nanoparticles; PLGA, poly (D, L-lactide-co-glicolide).

Materials and methods

Materials

DOX was procured from Tokyo Chemical Industry Co. Ltd, Japan. PLGA, 50:50 was obtained as a kind gift from Purac Biomaterials (Netherlands). Lecithin (98%) was acquired from Sigma Aldrich (St. Louis, MO, USA). DSPE-PEG 2000 was procured as research sample from the Lipoid GmbH (Ludwigshafen, Germany). Hank's balance salt solution (HBSS), trypsin (2.5%), Dulbecco's Modified Eagle Medium (DMEM), phosphate buffered saline (PBS), Rosewell Park Memorial Institute (RPMI), L-glutamine (200 mM), fetal bovine serum (FBS, 10%), non-essential amino acids (NEAA), and penicillin-streptomycin (PEST) were all procured from HyClone (USA). American Type Culture Collection provided all the required cell lines used in the present study. Freshly prepared Milli-Q water (Merck Millipore, USA) was used

in the preparation of formulation and buffers. All the other necessary chemicals and reagents used in the study were of analytical grade, and all solvents were of HPLC grade.

Preparation of doxorubicin base

Before the preparation of the LPHNPs, the DOX.HCl was converted into the hydrophobic base by extraction method. Briefly, a calculated amount of the DOX.HCl was dissolved in 5 mL of the Milli-Q water with continuous stirring; 01 mL of 0.2 M of sodium bicarbonate was added and mixed thoroughly for 5 minutes. The mixture was transfer into a separating funnel followed by the addition of chloroform. The chloroform layer was collected and the process repeated twice. Lastly, the organic solution was evaporated by rotary evaporator to get the DOX base.

Fabrication of the LPHNPs

NP formulations were produced by modified single step nanoprecipitation process, using the DOX.HCl, DOX base, PLGA, lecithin, and DSPE-PEG 2000 as structural components. Briefly, the organic phase containing polymer was prepared with a specific concentration (2 mg/mL) in acetonitrile. While the solution of lecithin and DSPE-PEG 2000 in a mass ratio of 2:3 in 4% of hydroethanolic solution constitute the aqueous phase. The amount of added lipid was 20% of the total weight of the PLGA used in the organic phase. The aqueous phase was heated at 65°C so that all the lipids melt and properly disperse in the hydroethanolic solution constituting the uniform aqueous phase. The final dispersion was prepared by the addition of organic phase in dropwise manner in the hydroethanolic solution in a 1:9 v/v ratio, by using the syringe pump under gentle stirring. Finally, the LPHNPs were purified and washed twice with Milli-Q water by centrifugation to remove the unentrapped drug and organic solvents. The above-mentioned procedure was also applied to fabricate the drug loaded LPHNPs. The specific amount of the DOX.HCl was added into the hydroethanolic phase, whereas the DOX base was dissolved into the organic solvent.

Characterization of the LPHNPs

Morphology

Transmission electron microscope imaging was employed to evaluate the shape and surface morphology of the fabricated LPHNPs. TEM analysis was performed by depositing the sample particles on the 400 mesh carbon coated copper grids using the negative staining approach.[15] Briefly, the dispersion of the LPHNPS was deposited on the TEM grid by placing the drop of sample NPs for specific time interval. Finally the grid was stained with negative stain (2% uranyl acetate), dried, and then visualized at a voltage of 120 kV by using TEM (Jeol JEM-1400, Jeol Ltd, Tokyo, Japan).[16]

Particle size, zeta-potential, and size distribution analysis

Malvern ZetaSizer Nano ZS instrument (Malvern Instruments Ltd, Malvern, UK) was employed to evaluate the mean particle size, particle size distribution, and zeta-potential of prepared nanoformulations. The dynamic light scattering (DLS) method indicates the *z*-average and polydispersity (PDI) of NPs in blank and drug loaded LPHNP formulations. The zeta-potential analysis used an electrophoretic mobility approach.[17]

Encapsulation efficiency

The direct measurement of the fluorescence of DOX in the sample was utilized for the calculation of the amount of drug encapsulated in all LPHNP formulations at 480 nm to 560 nm as excitation and emission wavelengths, respectively, because of the florescent nature of the DOX using the fluorescent detector (Thermo Fisher Scientific Inc., Waltham, MA, USA). The indirect method was employed using the supernatant to calculate the unentrapped DOX in the formulation. Finally, the amount of the encapsulated DOX was determined by using the following formula.

$$\%\,\mathrm{E.E} = \frac{\text{Amount of DOX loaded in LPHNPs}}{\text{Total amount of DOX added in formulation}} \times 100 \quad (1)$$

Drug release and kinetics

The membrane dialysis approach was used to evaluate the in vitro drug release from LPHNPs that simulate the ultimate performance of the DDS in the biological fluids. Briefly, an accurately calculated amount of NPs which encapsulated a fixed amount of DOX.HCl and DOX base were dispersed in the 1 mL of dissolution media (PBS pH 7.4), and this was put into the respective dialysis bags with 10–12 kDa average cutoff molecular weight. The dialysis bags were sealed with clips and placed in 40 mL of dissolution medium to study the release of the DOX for 24 hours The dialysis bags were placed on a magnetic stirrer at controlled temperature with a gentle shaking rate of 150 rpm. Then 200 µL of the sample was withdrawn and added in the 96-well plates at different predetermined time intervals (0, 0.25,

0.5, 0.75, 1, 2, 3, 4, 5, 6, 8, and 24 hours) in triplicate manner. After each sample, the same amount of the fresh dissolution medium maintained at the same temperature was added to keep the amount of dissolution medium constant throughout the experiment. The amount of the DOX released from the LPHNPs was determined by calculating the total fluorescence of the drug in the sample by Varioskan Plate reader at 480 nm and 560 nm as excitation and emission wavelengths, respectively.

The kinetics analysis of the DOX released from the LPHNPs was determined by incorporating the resultant data into various mathematical models. The regression coefficients (R^2) values will indicate the best fit model.

Fourier transform infrared (FTIR) spectroscopy

The interaction among the drug and the formulation components is significantly important to determine the efficacy and stability of the formulation. Solid state analysis was employed to determine the compatibility among the various components used in the present study. First, FTIR spectra of all the pure ingredients, drug, their physical mixtures, blank, and DOX loaded NPs were recorded by using FTIR and analysis for the characteristic peaks and their shift in individual to formulation spectra using OPUS 5.5 software. All the spectra were recorded from 3,500 to 500 cm^{-1} wavelength, with 4 cm^{-1} resolution and 64 scans.

Differential scanning calorimetry (DSC)

All the individual ingredients, their physical mixture, and the LPHNPs were analyzed by DSC to identify the solid state of the entrapped drug within the NPs. The DSC thermograms were recorded using the calorimeter that is previously standardized for the temperature and rate of heat flow by using Indium (melting point=157.6°C) as reference standard throughout the experiment (DSC 823e, Mettler Toledo, USA). Briefly, the accurately weighed samples were packed in the aluminum pans. Then the samples were analyzed by heating the samples from 25 to 250°C at 10°C/min linear heating rate with constant flow of the nitrogen that create an inert environment. The measured data was evaluated by STARe software.

Colloidal stability of LPHNPs

To evaluate the possible in vivo behavior, the stability of the prepared nanoparticles was determined in FBS, RPMI, and DMEM;100 mg of the powdered NPs were dispersed in the 2 mL of the respective solution and keep at 37°C under constant stirring of 100 rpm; 200 µL of each sample was collected at constant periods of time intervals and analyzed by using the Zetasizer Nano ZSP (Malvern Instruments) for any change in the particle size, polydispersity, and zeta-potential. All the data was collected from three independent experiments and expressed graphically.

Cell culturing

The various cancer cells (breast and prostate cancer) were grown separately in DMEM and RPMI culture media at 37°C, and 95% humidity with 5% CO_2 in a gas incubator (BB 16 gas incubator, Heraeus Instruments GmbH). Both the cell culture media were supplemented with 10% FBS, 1% NEAA, and 1% PEST. Before every test, the cells were unthaw, subcultured at 80% confluency, and seeded for further experiments.

In vitro cytotoxicity studies

The viability assay of all the selected LPHNPs was performed to access the in vitro cytotoxicity and nanoformulations. The ATPase activity based viability kits were used to measure the viable cells.[18] Briefly, the cells were grown and seeded by using the aforementioned protocol. An accurately weighed amount of the NPs were dispersed in the growth media to prepare all the samples, with concentrations ranging from 50–300 µg/mL. Cells were grown for proper attachment to the wall of the plate. Later, the cells were washed with the buffer and incubated with all the samples for the required period of time in 96-well plates. After incubation, the plates were equilibrated for 30 minutes at ambient temperature. Finally, the cells were washed with HBSS-HEPES buffer and treated with 50 µL CellTiter-Glo® (Luminescent Cell Viability Assay, Promega Corporation, USA) and 50 µL buffer in each well. The reagent was mixed properly with the cells by placing the plate on the orbit shaker for 2 minutes. The samples were placed in the Varioskan plate reader (Thermo Fisher Scientific Inc.) to measure the luminescence, which is directly correlated with the number of viable cells in the samples. All the results were taken as three independent readings and compared with negative and positive controls.

Cell uptake study

Cell internalization analysis is a valuable index to measure the ability of drug to enter in the cell and the concentration inside the cells. For the qualitative analysis of the cell internalization, human prostate and breast cancer cells were seeded and grown into a Lab-tek™ 8-chambered glass plate. Then 200 µL of the cells were added in each chamber and grown overnight for the

proper attachment with the chamber.[19] The cells were washed, treated with the 200 µL of DOX.HCl and DOX base loaded LPHNPs suspension, and incubated under the aforementioned growth conditions. Cells incubated without the NPs in the medium were considered as negative controls. Finally, the cells incubated with the samples were washed and stained by the following protocol. Briefly, the staining of cell membranes and nuclei was achieved by incubating the cells with 200 µL of DAPI (Thermo Fisher Scientific) and CellMask Deep Red (Life Technologies, US) for 5 and 3 minutes at 37°C, respectively. The excess of staining reagent was removed by washing and all the cells were fixed with 4% paraformaldehyde (PFA) for 15 minutes. The fixed cells in fresh buffer (pH 7.4) were analyzed by using a Leica inverted SP5 confocal microscope using HeNe (590 nm), Ar (488 nm), and HeNe (633 nm) lasers for the intracellular internalization of the LPHNPs and the drug molecules.

Antiproliferative assay

The antiproliferative action of pure drug solution, DOX.HCl, and DOX base loaded LPHNPs were determined by the cell proliferation experiments against the breast and prostate cancer cells. Briefly, all the cell were grown in accordance with the previously mentioned cell culturing protocol and incubated for attachment for 24 hours at a specific temperature. After incubation and attachment, the cells were washed and grown with the free drug solution, and the drug loaded LPHNPs suspension with different concentrations (ranging from 5 µg/mL to 200 µg/mL for all the three type of formulations) and incubated for the preselected time intervals. The live cell count was determined by using the viability assay kit (CellTiter-Glo®, Promega Corporation, USA) and the sample plates were analyzed for the luminescence in a Varioskan luminescence plate reader.

Statistical analysis

All the experimental data of the present study was presented as the result ± standard deviation. All the test results were taken in triplicate under same experimental conditions. The significance of different results was calculated by using the ANOVA.

Results and discussion

Morphology

TEM images of DOX.HCl and DOX base loaded LPHNPs are shown in Figure 2. All the formulations showed round, smooth surfaced, and nanosized particles. The inner bright portion of the NPs might indicate the presence of polymeric core encapsulating the drug. It is also evident that the drug loaded NPs maintained the uniform shape and surface with a slight increase in the size of the particles in agreement with previous studies. The TEM images of the blank LPHNPs (Figure 2C and D) indicate that there is no such bright cores are the present in the lipid coating that support the abovementioned results.[20]

Particles size, size distribution, and zeta-potential

The DLS method was employed to determine the size of the NPs. The blank LPHNPs were of 173.9±2.4 nm, which was slightly less than the particle size of drug loaded LPHNPs (182–208 nm) with a value of monodispersity (less the 0.16), as presented in Table 1. It was observed that the LPHNPs loaded with DOX base were relatively smaller (up to 185 nm) in size as compared to DOX.HCl loaded nanoparticles (up to 208 nm) (Table 1). The results suggest that there are smaller NPs formed with an increase in the hydrophobicity of the chemical constituents that might develop a better electrostatic and steric repulsion between the LPHNPs.[21] This size range is desirable for prolonged circulation and enhanced cell

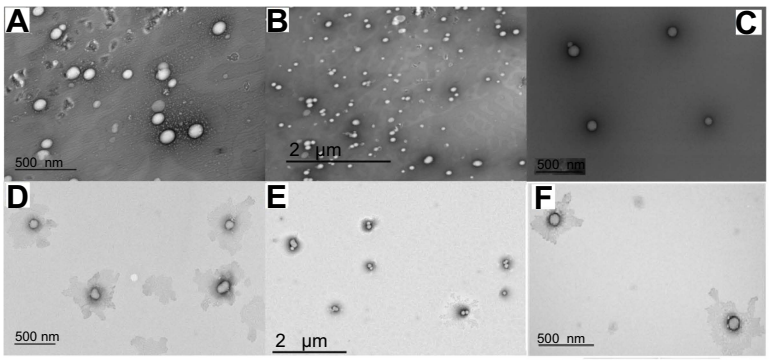

Figure 2 TEM images of DOX.HCl (**A** and **B**), Blank LPHNPs (**C** and **D**), and DOX base (**E** and **F**) loaded LPHNPs.
Abbreviations: DOX, doxorubicin; DOX.HCl, doxorubicin hydrochloride; LPHNPs, lipid polymer hybrid nanoparticles; TEM, transmission electron microscopy.

Table 1 Size, polydispersity (PDI) and zeta-potential of different prepared formulations

Sample code	Particle size (nm)	PDI	Zeta-potential (mV)
F_{H1}	204.8±1.4	0.050±0.007	−31.7±1.2
F_{H2}	207.5±1.0	0.089±0.021	−29.8±0.8
F_{H3}	201.4±3.1	0.085±0.031	−28.8±0.6
F_{B1}	182.4±1.0	0.183±0.037	−32.5±0.6
F_{B2}	183.8±0.8	0.153±0.015	−32.0±0.9
F_{B3}	185.8±3.2	0.154±0.240	−29.6±1.7
F_{Blank}	173.9±2.4	0.069±0.016	−28.0±0.1

uptake.[22] All the formulations showed negative zeta-potential (−31.7 to −28.0 mV) due to the presence of negatively charge lecithin, and their lipophilic properties in the NP matrix. This range of zeta-potential provides adequate repulsion between NPs and prevents aggregation in the liquid media, leading to good colloidal stability, as suggested by the previously published data.[23]

Encapsulation efficiency

The encapsulation efficiency (%EE) of DOX.HCl and DOX base loaded LPHNPs was measured by a direct method. From the data presented in Table 2, it is evident that the encapsulation is directly proportional to the amount of the polymer as compared to drug. Interestingly, the EE of the DOX base was higher as compared to the DOX.HCl at the constant amount of drug and polymer. The increased hydrophobicity of the drug proportional to EE and drug might be the reason for the increase in the overall entrapment efficiency of the system. It was also supported by the previous studies that the solubility in the aqueous medium and their interaction with the lipid component of the formulation. The Hydrophobic drug easily partitioned between the lipid layers as compared to the hydrophilic DOX.HCl that lead to a higher encapsulation of the hydrophobic drug as compared to the hydrophilic DOX.HCl.[24,25]

Table 2 Entrapment efficiency (EE) and percentage of drug release of the different prepared formulations

Sample code*	Drug/polymer ratio	Entrapment efficiency	% Drug release
*F_{H1}	1:5	17.80±1.91	53.23
*F_{H2}	1:10	30.11±1.17	56.72
*F_{H3}	1:20	43.80±4.36	48.76
**F_{B1}	1:5	40.32±0.60	33.29
**F_{B2}	1:10	52.87±0.34	35.57
**F_{B3}	1:20	59.78±1.35	32.93

Note: *Formulations F_{H1}–F_{H3} were LPHNPs loaded with DOX.HCl, while **F_{B1}–F_{B3} were loaded with DOX base.
Abbreviations: DOX, doxorubicin; DOX.HCl, doxorubicin hydrochloride; LPHNPs, lipid polymer hybrid nanoparticles.

Drug release and kinetics

The in vitro drug release studies were performed using a dialysis bag method in PBS (pH 7.4) dissolution medium. The amount of drug released from the NPs is shown in Table 3. All formulations showed a biphasic drug release pattern. However, the release of DOX.HCl was relatively faster than DOX base. Lesser aqueous solubility and high association with the lipid components might contribute to controlled release of DOX base from the prepared LPHNPs.[26,27] The better solubility of the DOX.HCl in the aqueous media lead to rapid diffusion of the drug molecules from the LPHNPs, as compared to the DOX base loaded formulations. Moreover, due to the hydrophobic nature of the lipid, the aqueous media access is limited towards the nanoparticles. In addition to that, the DOX base is a highly hydrophobic one, which releases from the formulation very slowly in the given period of release studies. In the kinetic analysis, the values of the correlation coefficient and diffusional coefficient (n) (Table 3), indicating that all the NPs containing DOX.HCl and DOX base follow the Fickian diffusion ($n<0.5$) mechanism of release from the LPHNPs with the Higuchi (R^2=0.9867–0.9450) kinetic model.[28,29]

Fourier transform infrared (FTIR) study

Previously, we conducted a comprehensive study to evaluate the compatibility and presence of any possible physical and/or chemical incompatibility between the different structural components of DDS.[30] In this study, the characteristic FTIR spectra of all pure chemicals, blank and DOX loaded LPHNPs were also recorded, as shown in Figure 3. The FTIR spectra of DOX in Figure 3D indicates the characteristic bands at 3,320 cm^{-1} (N-H asymmetric stretching), and 2,935 cm^{-1} (C-H stretching vibration). The band at 1,730 cm^{-1} shows the presence of the C-O group,[31] whereas distinct bands at 1,615 cm^{-1} and 1,580 cm^{-1} correspond to the bending vibration of amide I and amide II groups, respectively, that overlap with the carbonyl groups of the anthracene ring.[32,33] The IR spectra of PLGA (Figure 3A) indicate the characteristic bands at 2,995 cm^{-1} and 2,946 cm^{-1}, specifying the -C-H symmetrical stretching at C-H and methyl $(CH)_3$ group associated with the lactic acid monomer of PLGA, while distinct bands located at 1,452 and 1,423 cm^{-1} indicate the occurrence of a glycolic acid fraction of the polymer.[34] The sharp band at 1,747 cm^{-1} corresponds to

Table 3 Kinetic modeling of drug release of different prepared formulations after data fitting in different kinetic models

Formulations	Zero order		First order		Higuchi model		Korsmeyer-Peppas model	
	R^2	K_o	R^2	K	R^2	K_H	R^2	N
*F_{H1}	0.8997	4.0231	0.8039	0.0596	0.9867	23.8213	0.9891	0.4366
*F_{H2}	0.7922	2.9944	0.6979	0.0685	0.9542	25.9411	0.9485	0.4061
*F_{H3}	0.7529	1.8092	0.6825	0.0443	0.9366	24.3306	0.9416	0.3388
**F_{B1}	0.8705	2.2866	0.7752	0.0888	0.9699	15.4400	0.9703	0.4013
**F_{B2}	0.8763	1.7382	0.7393	0.0702	0.9611	14.4618	0.9600	0.4619
**F_{B3}	0.8942	1.547	0.7905	0.0853	0.9450	10.7767	0.9442	0.3989

Note: *Formulations F_{H1}–F_{H3} were LPHNPs loaded with DOX.HCl, while **F_{B1}–F_{B3} were loaded with DOX base.
Abbreviations: DOX, doxorubicin; DOX.HCl, doxorubicin hydrochloride; LPHNPs, lipid polymer hybrid nanoparticles.

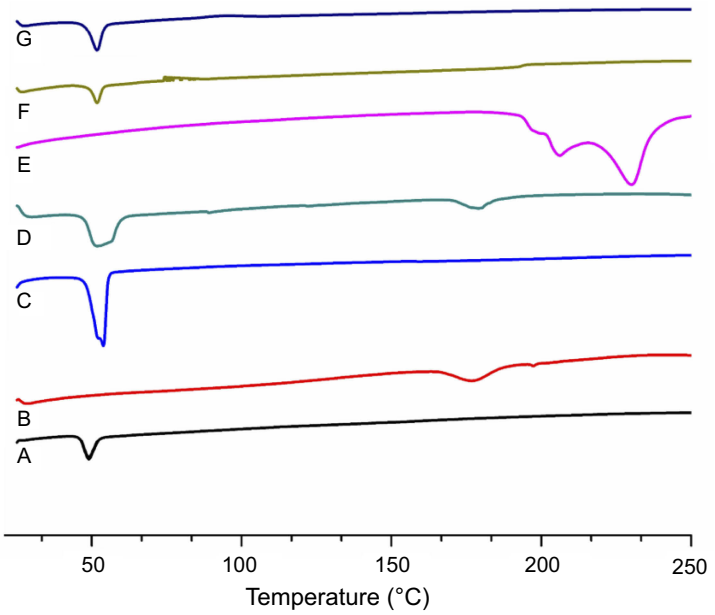

Figure 3 FTIR spectra of PLGA (**A**), lecithin (**B**), DSPE-PEG 2000 (**C**), Luterol (**D**), DOX (**E**) blank formulation (**F**), and DOX loaded LPHNPS (**G**).
Abbreviations: DOX, doxorubicin; DSPE-PEG 2000, 1,2-distearoyl-Sn-glycero-3-phosphoethanolamine-N-[methoxy (polyethylene glycol)]-2000; LPHNPs, lipid polymer hybrid nanoparticles; PLGA, poly (D, L-lactide-co-glicolide).

the ester carbonyl group symmetric stretching (-C=O).[35] The spectra of the physical mixture demonstrate the characteristic bands of all the individual components without any remarkable shift from the normal position. The FTIR spectra of blank LPHNPs (Figure 3E) indicate the presence of distinct bands of the PLGA and lecithin, which is supported by the data in different studies.[36,37] The data suggest that there was no significant shift in the pattern of peaks of the polymer and lipid in the FTIR spectra of blank LPHNPs that strengthen the lack of any possible physical and chemical interactions with the loaded drug molecules. The slight shift of distinct bands of DOX at 3,268 cm^{-1} and 3,270 cm^{-1}, demonstrating N-H stretching of drug in the prepared formulations, was not observed in the IR spectra of blank LPHNPs (Figure 3F). However, intense signals of the carbonyl (C=O) group show a slight shift in wave number at 1,753 cm^{-1}, which might be due to the overlapping of identical groups in lecithin and PLGA.[38]

Differential scanning calorimetry (DSC) analysis

Thermal analysis was performed to determine any possible change in physical characteristics of the formulation components individually and to evaluate crystalline or amorphous behavior of the DOX loaded in the LPHNPs. The phase transition studies might indicate the changes in the crystallinity of the drug that affect the in vitro drug discharge process and in vivo cellular

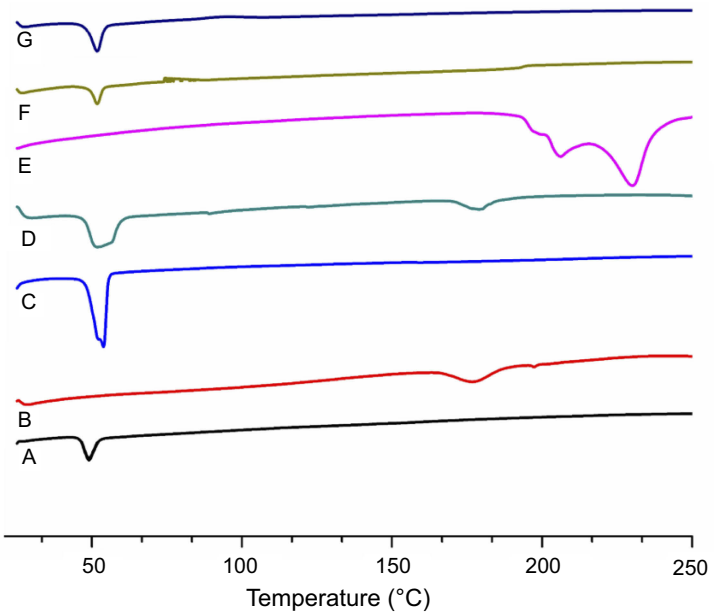

Figure 4 DSC thermograms of PLGA (**A**), lecithin (**B**), DSPE-PEG 2000 (**C**), physical mixture (**D**), DOX (**E**), blank LPHNPs (**F**) and DOX loaded LPHNPS (**G**).
Abbreviations: DOX, doxorubicin; DSC, differential scanning calorimetry; DSPE-PEG 2000, 1,2-distearoyl-Sn-glycero-3-phosphoethanolamine-N-[methoxy (polyethylene glycol)]-2000; LPHNPs, lipid polymer hybrid nanoparticles; PLGA, poly (D, L-lactide-co-glicolide).

uptake.[39] Different combinations of the structural components and drug might exist, like the amorphous drug and the crystalline structure of the polymer. Figure 4 shows the thermograms of pure DOX, PLGA, lecithin, physical mixture, and drug loaded LPHNPs. A PLGA thermogram (Figure 4A) shows a characteristic peak at 50°C that correlates with the glass transition temperature of the polymer and is not affected by the formulation procedure.[40,41] A DSC thermogram of DOX presents a typical endothermic melting peak ca 220°C, demonstrating the crystallinity present in the DOX molecular structure (Figure 4E). However, a broad and slightly shifted peak was observed in the physical mixture (Figure 4D), and no such peak was identified in the DSC thermogram of the LPHNPs (Figure 4G), indicating that either the drug is completely loaded inside the core material or loses its crystalline structure due to structural deformations.[42] The results indicated the change of the physical state of the drug during the NPs formulation.[43,44] It is suggested that the conversion from crystalline to amorphous phase increases the drug saturation solubility and inhibits the Ostwald ripening phenomenon.[45] It was also revealed from the data that there was no significant change in the characteristic peaks of all the structural components in the LPHNPS thermograms, confirming the compatibility among the drug and formulation components. Thus, all these factors suggest that these LPHNPs formulations show better stability and in vivo performance.[46]

Colloidal stability of LPHNPs

The colloidal stability of the fabricated LPHNPs was explored in PBS, DMEM, and RPMI, which is an indication of biocompatibility and safety after in vivo use of these LPHNPs. The findings of particle size, PDI, and zeta-potential revealed good stability (Figure 5). LPHNPs showed slightly larger sized particles in DMEM and RPMI media that might be due to the interaction between the NPs and the proteins present in the growth media. The negatively charged surface of LPHNPs offered excellent physical stability to these nanocarriers that is an indication of their suitability for further evaluation.[16,29]

Cell viability studies

The investigation of the toxicity profile of the drug delivery system is of prime importance in the translation for biomedical applications.[19] The biocompatibility and viability were evaluated in MDA-MB-231 and PC3 cells at various concentrations (up to 300 μg/mL) of the LPHNPs and exposure time. The main aim of using various concentrations was to evaluate the dose or concentration dependent toxicity and the maximum safe concentration of LPHNPs that might be administered for

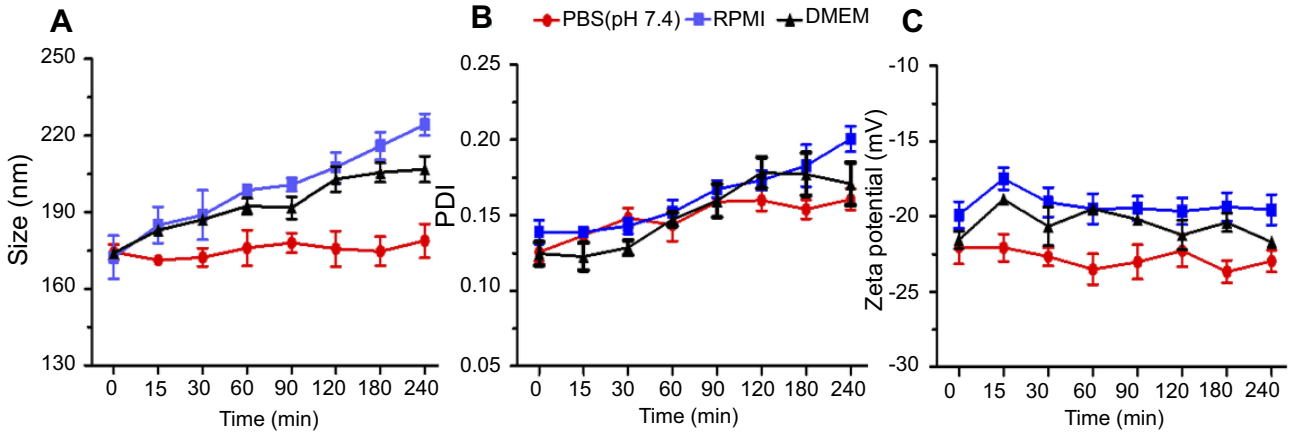

Figure 5 Colloidal stability studies, indicating the variation in particle size (**A**), PDI (**B**), and zeta-potential (**C**) in PBS, DMEM, and RPMI up to 4 hours at 37°C. All the results are presented in triplicate, along with error bars, as mean±SD (n=3).
Abbreviations: DMEM, Dulbecco's Modified Eagle Medium; PBS, phosphate buffered saline; PDI, polydispersity; RPMI, Rosewell Park Memorial Institute.

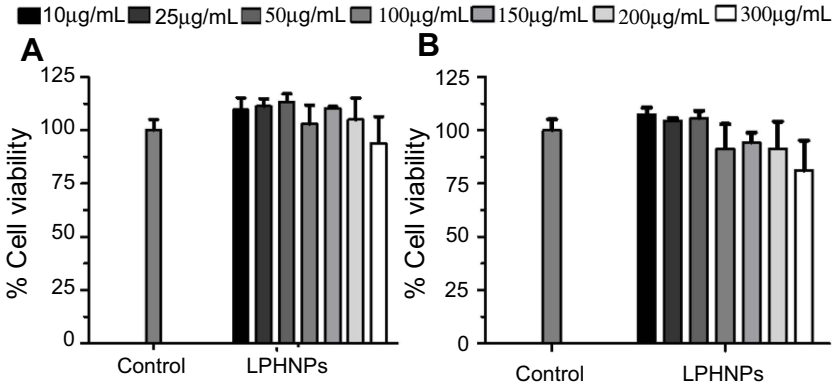

Figure 6 Cell viability study of the blank LPHNPs after 24 hours (**A**) and 48 hours (**B**) incubation with MDA-MB-231 cells at 37°C. The results are presented in triplicate with error bars as mean±SD (n=3).
Abbreviation: LPHNPs, lipid polymer hybrid nanoparticles.

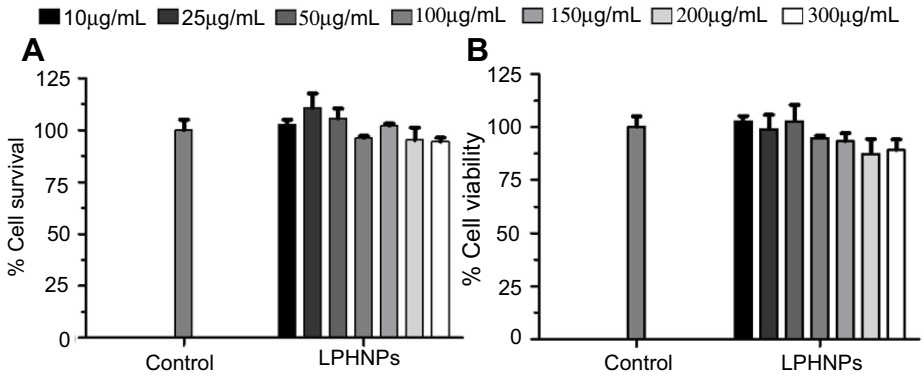

Figure 7 Cytotoxicity study of LPHNPs measured after 24 hours (**A**) and 48 hours (**B**) incubation with PC3 cells at 37°C. The results are presented in triplicate, with error bars as mean±SD (n=3).
Abbreviation: LPHNPs, lipid polymer hybrid nanoparticles.

the clinical application of these NPs. The particles were evaluated for two different incubations periods, 24 and 48 hours, and the results are shown in Figures 6 and 7. After the selected time period no cytotoxicity was observed, as the viability of both type of cells was approximately 100% at all tested doses, being similar to the control sample.

Similarly, no significant cell death was observed after 48 hours, even at the highest concentration (300 µg/mL) of the LPHNPs. Our findings are supported by various studies confirming the safe nature of the LPHNPs and elaborating no significant toxic effects.[47–49]

Cell uptake study

The extent of cellular internalization of the NPs and the intracellular drug release are two main indicators of the drug delivery potential of a nanocarrier system. DOX hydrochloride and DOX base loaded LPHNPs were incubated (at a concentration of 25 µg/mL of the DOX in the LPHNPs and the free drug solution) with cancer cells, and the internalization of NPs was investigated using confocal fluorescence imaging at 37°C. Due to the fluorescent nature of the DOX itself, no other fluorescence dye was loaded into the NPs; however, for the fluorescence imaging, the cells were stained with DAPI and CellMask Deep Red to identify the nuclei and cell membranes, respectively (Figure 8). The LPHNPs showed a dose and time dependent cell internalization through the cell membranes that might follow the endocytosis pathway. Initially, the fluorescence signals of the drug inside the cell were relatively weak as compared to the signals at higher concentration. It was also found that the fluorescence signals of the DOX.HCl LPHNPs were mainly localized at inner and outer compartments of the cells membrane. Moreover, the intense fluorescence signals of DOX loaded LPHNPs were observed in the inner cytoplasmic region, and even early/fast uptake was identified in the nuclei. The results suggest that the presence of lipid coating simulates with cell membranes structure that would facilitate the uptake of these NPs.[50] However, the NPs loaded with the hydrophilic form of the DOX had less uptake, which may also be followed by the rapid efflux from the cells due to less permeability and rapid release from the NPs. The results are further supported by the previous data that demonstrated that the physical

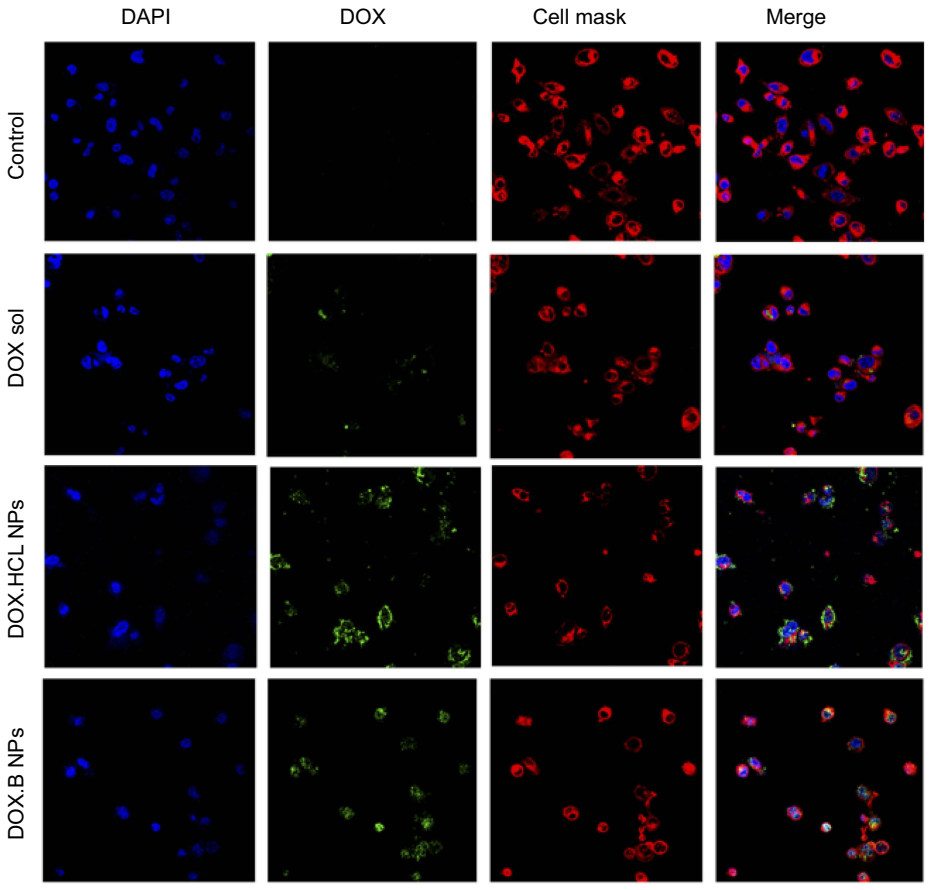

Figure 8 Confocal microscopic images of LPHNPs containing DOX solution. DOX.HCl and DOX base growing for 24 hours at 37°C in breast cancer cells. DAPI (blue) and CellMask Deep Red (red) were used to stain the different components of the cell. Green signals indicate the presence of DOX in the cells.
Abbreviations: DOX, doxorubicin; DOX-HCl, doxorubicin hydrochloride; LPHNPs, lipid polymer hybrid nanoparticles.

binding of DOX with cell membrane lipids produced higher cellular internalization and retention inside the cellular compartments.[51,52] The loading of DOX.HCl and the DOX into the polymersomes by Xu et al[21] also support our finding by describing the effect of hydrophilicity and hydrophobicity on the cytotoxic effects and cell permeation in the MCF-7 cells and demonstrated the higher uptake of the lipophilic DOX. It was also established that NPs with particle sizes of ≤200 nm might improve the cellular uptake and intracellular concentration of the loaded drug by enhanced permeability and retention effects that ultimately enhanced the therapeutic efficacy.[53]

Antiproliferative assay

The antiproliferative effects of both formulations were evaluated and compared with the drug solution in MDA-MB-231 human breast cancer cells and PC3 human prostate cancer cells. The results indicate the concentration and time dependent antiproliferative effects with pure DOX solution and LPHNPs, containing the DOX.HCl and lipophilic DOX base, respectively (Figures 9 and

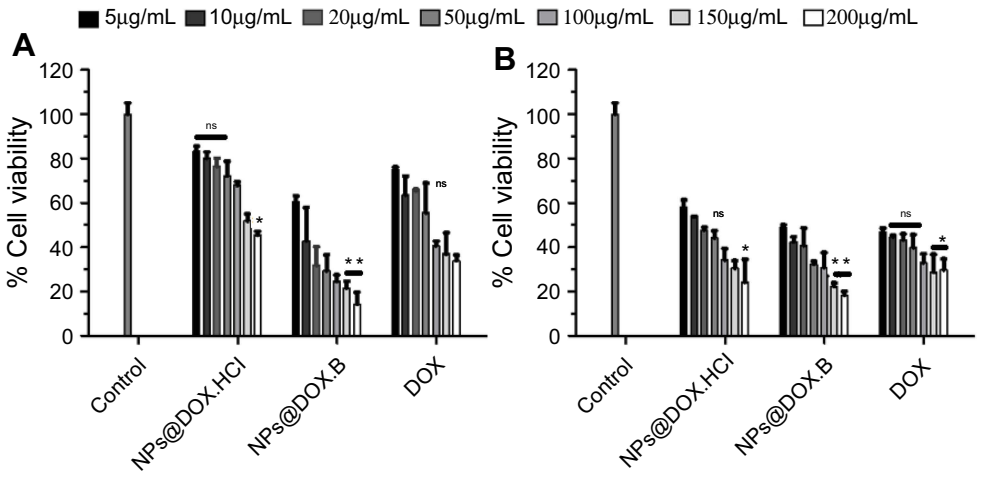

Figure 9 Cell growth inhibitory effects of the DOX solution, DOX.HCl loaded LPHNPs and DOX base loaded LPHNPs measured after 24 hours (**A**) and 48 hours (**B**) incubation along MDA-MB-231 cells. The activity was determined by CellTiter Glo viability assay. Results are presented with error bar, indicating mean±SD (n=3). *Significant where *P*>0.05, **significant where *P*>0.01.

Abbreviations: DOX, doxorubicin; DOX-HCl, doxorubicin hydrochloride; LPHNPs, lipid polymer hybrid nanoparticles; ns, non-significance.

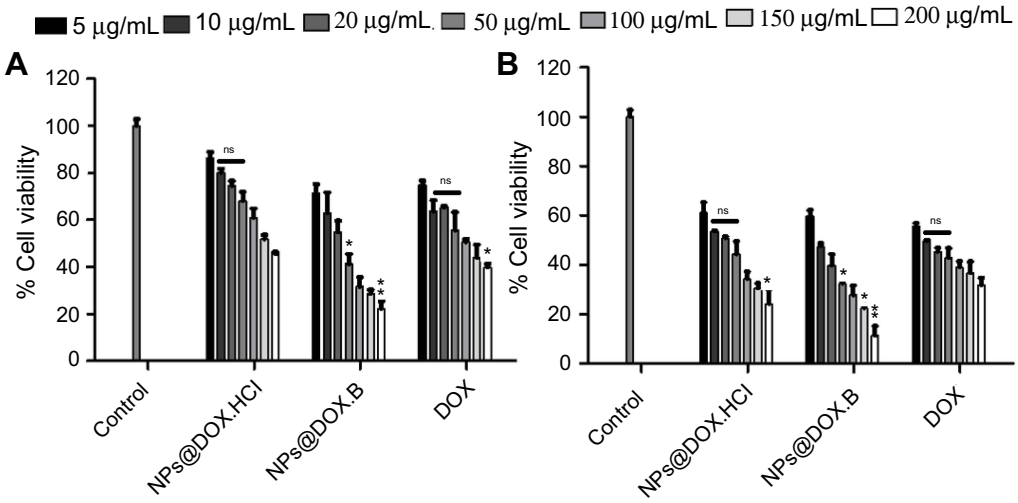

Figure 10 Cell growth inhibitory effects of the DOX solution, DOX.HCl loaded LPHNPs and DOX base loaded LPHNPs measured after 24 hours (**A**) and 48 hours (**B**) incubation along PC3 cells. The activity was determined by CellTiter Glo viability assay. Results are presented with error bar, indicating mean±SD (n=3). *Significant where *P*>0.05, **significant where *P*>0.01.

Abbreviations: DOX, doxorubicin; DOX-HCl, doxorubicin hydrochloride; LPHNPs, lipid polymer hybrid nanoparticles; ns, non-significance.

10). The results also indicate the encapsulation of the DOX inside the LPHNP, which retained its antitumor activity and was significantly higher compared to the pure drug solution. The higher activity was due to the greater uptake of the LPHNPs in the cell. The findings are supported by previous studies that indicated the incorporation of the DOX within the lipid polymer hybrid system hindered efflux and rapid removal of the DOX from the cells.[54,55] Another important finding is the higher antiproliferative effect of lipophilic DOX base compared to the DOX.HCl, due to the hydrophobic interaction between LPHNP components and the DOX that improves the permeability and penetration of the LPHNPs across the cell membranes.[51,56]

Conclusions

In this study, we successfully fabricated DOX.HCl and DOX base loaded LPHNPs by the modified single step nanoprecipitation method and evaluated different physicochemical properties. The particle size analysis indicated the LPHNPs with a size range of 174–208 nm have good dispersity (PDI<0.3). The particles showed higher encapsulation of DOX base (59.8±1.4) compared to DOX.HCl (43.8±4.4) due to its lipophilic nature. The LPHNPs loaded with DOX base provide slower drug release (32.9%) as compared to DOX.HCl after 24 hours. The FTIR and DSC analysis showed the physicochemical compatible of the particles and its components. Moreover, the in vitro viability and cell internalization studies indicated better safety, enhanced antitumor effect, and cell uptake. These characteristics may endow LPHNPs improved therapeutic effects in the tumor microenvironment. Altogether, the LPHNPs provide a significantly important DDS chemotherapeutic delivery for future anti-cancer applications.

Acknowledgments

We acknowledge the International Research Support Initiative Program (IRSIP) of the Higher Education Commission of Pakistan for the travel grant for the University of Helsinki Finland, the indigenous PhD scholarship from Higher Education Commission of Pakistan, financial support from the Sigrid Jusélius Foundation (Decision No. 4704580), and the Helsinki Institute of Life Science Research Funds. The Electron Microscopy Unit of the University of Helsinki is acknowledged for providing the facilities for TEM imaging, and the Light Microscopy Unit of the Institute of Biotechnology for the instrumentation for confocal microscopy.

Disclosure

The authors report no conflicts of interest in this work.

References

1. Badr G, Al-Sadoon MK, Rabah DM. Therapeutic efficacy and molecular mechanisms of snake (Walterinnesia aegyptia) venom-loaded silica nanoparticles in the treatment of breast cancer-and prostate cancer-bearing experimental mouse models. *Free Radical Biol Med*. 2013;65:175–189. doi:10.1016/j.freeradbiomed.2013.06.018
2. Yip N, Fombon I, Liu P, et al. Disulfiram modulated ROS–MAPK and NFκB pathways and targeted breast cancer cells with cancer stem cell-like properties. *Br J Cancer*. 2011;104(10):1564. doi:10.1038/bjc.2011.126
3. Guo Y, Wang L, Lv P, Zhang P. Transferrin-conjugated doxorubicin-loaded lipid-coated nanoparticles for the targeting and therapy of lung cancer. *Oncol Lett*. 2015;9(3):1065–1072. doi:10.3892/ol.2014.2840
4. Yang H, Xu M, Li S, et al. Chitosan hybrid nanoparticles as a theranostic platform for targeted doxorubicin/VEGF shRNA co-delivery and dual-modality fluorescence imaging. *RSC Adv*. 2016;6(35):29685–29696. doi:10.1039/C6RA03843C
5. Ding D, Tang X, Cao X, et al. Novel self-assembly endows human serum albumin nanoparticles with an enhanced antitumor efficacy. *AAPS PharmSciTech*. 2014;15(1):213–222. doi:10.1208/s12249-013-0041-3
6. Wu B, Yu P, Cui C, et al. Folate-containing reduction-sensitive lipid–polymer hybrid nanoparticles for targeted delivery of doxorubicin. *Biomater Sci*. 2015;3(4):655–664. doi:10.1039/c4bm00462k
7. Kim BYS, Rutka JT, Chan WCW. Current concept: nanomedicine. *N Engl J Med*. 2010;363(25):2434–2443. doi:10.1056/NEJMra0912273
8. Gu L, Shi T, Sun Y, et al. Folate-modified, indocyanine green-loaded lipid-polymer hybrid nanoparticles for targeted delivery of cisplatin. *J Biomater Sci Polym Ed*. 2017;28(7):690–702. doi:10.1080/09205063.2017.1296347
9. Salvador-Morales C, Zhang L, Langer R, Farokhzad OC. Immunocompatibility properties of lipid–polymer hybrid nanoparticles with heterogeneous surface functional groups. *Biomaterials*. 2009;30(12):2231–2240. doi:10.1016/j.biomaterials.2009.01.005
10. Bose RJ, Ravikumar R, Karuppagounder V, Bennet D, Rangasamy S, Thandavarayan RA. Lipid–polymer hybrid nanoparticle-mediated therapeutics delivery: advances and challenges. *Drug Discovery Today*. 2017. doi:10.1016/j.drudis.2017.05.015
11. Liu Y, Liu J, Liang J, et al. Mucosal transfer of wheat germ agglutinin modified lipid-polymer hybrid nanoparticles for oral delivery of oridonin. *Nanomed*. 2017. doi:10.1016/j.nano.2017.05.003
12. Binaschi M, Bigioni M, Cipollone A, et al. Anthracyclines: selected new developments. *Curr Med Chem-Anti-Cancer Agents*. 2001;1(2):113–130.
13. Maluf F, Spriggs D. Anthracyclines in the treatment of gynecologic malignancies. *Gynecol Oncol*. 2002;85(1):18–31. doi:10.1006/gyno.2001.6355
14. Minotti G, Salvatorelli E, Menna P. Pharmacological foundations of cardio-oncology. *J Pharmacol Exp Ther*. 2010;334(1):2–8. doi:10.1124/jpet.110.165860
15. Argilés JM, Busquets S, Stemmler B, López-Soriano FJ. Cancer cachexia: understanding the molecular basis. *Nature Rev Cancer*. 2014;14(11):754. doi:10.1038/nrc3829
16. Tahir N, Madni A, Balasubramanian V, et al. Development and optimization of methotrexate-loaded lipid-polymer hybrid nanoparticles for controlled drug delivery applications. *Int J Pharm*. 2017. doi:10.1016/j.ijpharm.2017.09.061
17. Küçüktürkmen B, Devrim B, Saka OM, Yilmaz Ş, Arsoy T, Bozkir A. Co-delivery of pemetrexed and miR-21 antisense oligonucleotide by lipid-polymer hybrid nanoparticles and effects on glioblastoma cells. *Drug Dev Ind Pharm*. 2017;43(1):12–21. doi:10.1080/03639045.2016.1200069

18. Figueiredo P, Balasubramanian V, Shahbazi M-A, et al. Angiopep2-functionalized polymersomes for targeted doxorubicin delivery to glioblastoma cells. *Int J Pharm*. 2016;511(2):794–803. doi:10.1016/j.ijpharm.2016.07.066
19. Li W, Liu D, Zhang H, et al. Microfluidic assembly of a nano-in-micro dual drug delivery platform composed of halloysite nanotubes and a pH-responsive polymer for colon cancer therapy. *Acta Biomater*. 2017;48:238–246. doi:10.1016/j.actbio.2016.10.042
20. Sgorla D, Lechanteur A, Almeida A, et al. Development and characterization of lipid-polymeric nanoparticles for oral insulin delivery. *Expert Opin Drug Deliv*. 2018. (just-accepted). doi:10.1080/17425247.2018.1420050
21. Xu J, Zhao Q, Jin Y, Qiu L. High loading of hydrophilic/hydrophobic doxorubicin into polyphosphazene polymersome for breast cancer therapy. *Nanomed*. 2014;10(2):349–358. doi:10.1016/j.nano.2013.08.004
22. Zheng M, Yue C, Ma Y, et al. Single-step assembly of DOX/ICG loaded lipid–polymer nanoparticles for highly effective chemo-photothermal combination therapy. *ACS Nano*. 2013;7(3):2056–2067.
23. Celia C, Cosco D, Paolino D, Fresta M. Nanoparticulate devices for brain drug delivery. *Med Res Rev*. 2011;31(5):716–756. doi:10.1002/med.20201
24. Mu L, Feng S. A novel controlled release formulation for the anticancer drug paclitaxel (Taxol®): PLGA nanoparticles containing vitamin E TPGS. *J Controlled Release*. 2003;86(1):33–48.
25. Niu J, Wang A, Ke Z, Zheng Z. Glucose transporter and folic acid receptor-mediated Pluronic P105 polymeric micelles loaded with doxorubicin for brain tumor treating. *J Drug Target*. 2014;22(8):712–723. doi:10.3109/1061186X.2014.913052
26. Li Y, Wong HL, Shuhendler AJ, Rauth AM, Wu XY. Molecular interactions, internal structure and drug release kinetics of rationally developed polymer–lipid hybrid nanoparticles. *J Controlled Release*. 2008;128(1):60–70. doi:10.1016/j.jconrel.2008.02.014
27. Xu L, Xu S, Wang H, et al. Enhancing the efficacy and safety of doxorubicin against hepatocellular carcinoma through a modular assembly approach: the combination of polymeric prodrug design, nanoparticle encapsulation, and cancer cell-specific drug targeting. *ACS Appl Mater Interfaces*. 2018; 10(4):3229–3240.
28. Zhou Z, Kennell C, Jafari M, et al. Sequential delivery of erlotinib and doxorubicin for enhanced triple negative breast cancer treatment using polymeric nanoparticle. *Int J Pharm*. 2017;530(1–2):300–307. doi:10.1016/j.ijpharm.2017.07.085
29. Duan R, Li C, Wang F, Yangi J-C. Polymer–lipid hybrid nanoparticles-based paclitaxel and etoposide combinations for the synergistic anticancer efficacy in osteosarcoma. *Colloids Surf B*. 2017;159:880–887. doi:10.1016/j.colsurfb.2017.08.042
30. Tahir N, Madni A, Kashif PM, et al. Formulation and compatibility assessment of PLGA/lecithin based lipid-polymer hybrid nanoparticles containing doxorubicin. *Acta Poloniae Pharm- Drug Res*. 2017;74(5):1563–1572.
31. Amjad MW, Amin MCIM, Katas H, Butt AM, Kesharwani P, Iyer AK. In vivo antitumor activity of folate-conjugated cholic acid-polyethylenimine micelles for the codelivery of doxorubicin and siRNA to colorectal adenocarcinomas. *Mol Pharm*. 2015;12(12):4247–4258. doi:10.1021/acs.molpharmaceut.5b00827
32. Zhao X, Chen Q, Li Y, Tang H, Liu W, Yang X. Doxorubicin and curcumin co-delivery by lipid nanoparticles for enhanced treatment of diethylnitrosamine-induced hepatocellular carcinoma in mice. *Eur J Pharm Biopharm*. 2015;93:27–36. doi:10.1016/j.ejpb.2015.03.003
33. Nguyen CK, Tran NQ, Nguyen TP, Nguyen DH. Biocompatible nanomaterials based on dendrimers, hydrogels and hydrogel nanocomposites for use in biomedicine. *Adv Natural Sci*. 2017;8(1):015001.
34. Hosseininasab S, Pashaei-Asl R, Khandaghi AA, et al. Synthesis, characterization, and in vitro studies of PLGA–PEG nanoparticles for oral insulin delivery. *Chem Biol Drug Des*. 2014;84(3):307–315. doi:10.1111/cbdd.12318
35. Pirooznia N, Hasannia S, Lotfi AS, Ghanei M. Encapsulation of alpha-1 antitrypsin in PLGA nanoparticles: in vitro characterization as an effective aerosol formulation in pulmonary diseases. *J Nanobiotechnology*. 2012;10(1):20. doi:10.1186/1477-3155-10-20
36. Wang X, Luo Z, Xiao Z. Preparation, characterization, and thermal stability of β-cyclodextrin/soybean lecithin inclusion complex. *Carbohydr Polym*. 2014;101:1027–1032. doi:10.1016/j.carbpol.2013.10.042
37. Nagy K, Bíró G, Berkesi O, Benczédi D, Ouali L, Dékány I. Intercalation of lecithins for preparation of layered nanohybrid materials and adsorption of limonene. *Appl Clay Sci*. 2013;72:155–162. doi:10.1016/j.clay.2012.11.008
38. Kumar SSD, Mahesh A, Mahadevan S, Mandal AB. Synthesis and characterization of curcumin loaded polymer/lipid based nanoparticles and evaluation of their antitumor effects on MCF-7 cells. *Biochim Et Biophys Acta (Bba)-Gen Subj*. 2014;1840(6):1913–1922. doi:10.1016/j.bbagen.2014.01.016
39. Gandhi A, Jana S, Sen KK. In-vitro release of acyclovir loaded Eudragit RLPO® nanoparticles for sustained drug delivery. *Int J Biol Macromol*. 2014;67:478–482. doi:10.1016/j.ijbiomac.2014.04.019
40. Musumeci T, Ventura CA, Giannone I, et al. PLA/PLGA nanoparticles for sustained release of docetaxel. *Int J Pharm*. 2006;325(1):172–179. doi:10.1016/j.ijpharm.2006.06.023
41. Sanna V, Roggio AM, Pala N, et al. Effect of chitosan concentration on PLGA microcapsules for controlled release and stability of resveratrol. *Int J Biol Macromol*. 2015;72:531–536. doi:10.1016/j.ijbiomac.2014.08.053
42. Subedi RK, Kang KW, Choi H-K. Preparation and characterization of solid lipid nanoparticles loaded with doxorubicin. *Eur J Pharm Sci*. 2009;37(3):508–513. doi:10.1016/j.ejps.2009.04.008
43. Kalaria DR, Sharma G, Beniwal V, Ravi Kumar MNV. Design of biodegradable nanoparticles for oral delivery of doxorubicin: in vivo pharmacokinetics and toxicity studies in rats. *Pharm Res*. 2009;26(3):492–501. doi:10.1007/s11095-008-9763-4
44. Duan J, Mansour HM, Zhang Y, et al. Reversion of multidrug resistance by co-encapsulation of doxorubicin and curcumin in chitosan/poly(butyl cyanoacrylate) nanoparticles. *Int J Pharm*. 2012;426(1):193–201. doi:10.1016/j.ijpharm.2012.01.020
45. Lv Q, Yu A, Xi Y, et al. Development and evaluation of penciclovir-loaded solid lipid nanoparticles for topical delivery. *Int J Pharm*. 2009;372(1):191–198. doi:10.1016/j.ijpharm.2009.01.014
46. Akbarzadeh A, Mikaeili H, Zarghami N, Mohammad R, Barkhordari A, Davaran S. Preparation and in vitro evaluation of doxorubicin-loaded Fe3O4 magnetic nanoparticles modified with biocompatible copolymers. *Int J Nanomedicine*. 2012;7:511–526. doi:10.2147/IJN.S24326
47. Zhao X, Li F, Li Y, et al. Co-delivery of HIF1α siRNA and gemcitabine via biocompatible lipid-polymer hybrid nanoparticles for effective treatment of pancreatic cancer. *Biomaterials*. 2015;46:13–25. doi:10.1016/j.biomaterials.2014.12.028
48. Li F, Zhao X, Wang H, et al. Multiple layer-by-layer lipid-polymer hybrid nanoparticles for improved FOLFIRINOX chemotherapy in pancreatic tumor models. *Adv Funct Mater*. 2015;25(5):788–798. doi:10.1002/adfm.201401583
49. Yan J, Wang Y, Zhang X, Liu S, Tian C, Wang H. Targeted nanomedicine for prostate cancer therapy: docetaxel and curcumin co-encapsulated lipid–polymer hybrid nanoparticles for the enhanced anti-tumor activity in vitro and in vivo. *Drug Deliv*. 2016;23(5):1757–1762. doi:10.3109/10717544.2015.1069423
50. Liu Q, Zhang J, Sun W, Xie QR, Xia W, Gu H. Delivering hydrophilic and hydrophobic chemotherapeutics simultaneously by magnetic mesoporous silica nanoparticles to inhibit cancer cells. *Int J Nanomedicine*. 2012;7:999. doi:10.2147/IJN.S30631

51. Wong HL, Rauth AM, Bendayan R, Wu XY. In vivo evaluation of a new polymer-lipid hybrid nanoparticle (PLN) formulation of doxorubicin in a murine solid tumor model. *Eur J Pharm Biopharm*. 2007;65(3):300–308. doi:10.1016/j.ejpb.2006.10.022
52. Hu C-MJ, Kaushal S, Cao HST, et al. Half-antibody functionalized lipid− polymer hybrid nanoparticles for targeted drug delivery to carcinoembryonic antigen presenting pancreatic cancer cells. *Mol Pharm*. 2010;7(3):914–920. doi:10.1021/mp900316a
53. Maeda H, Nakamura H, Fang J. The EPR effect for macromolecular drug delivery to solid tumors: improvement of tumor uptake, lowering of systemic toxicity, and distinct tumor imaging in vivo. *Adv Drug Deliv Rev*. 2013;65(1):71–79. doi:10.1016/j.addr.2012.10.002
54. Prabhu RH, Patravale VB, Joshi MD. Polymeric nanoparticles for targeted treatment in oncology: current insights. *Int J Nanomedicine*. 2015;10:1001–1018. doi:10.2147/IJN.S56932
55. Prados J, Melguizo C, Ortiz R, et al. Doxorubicin-loaded nanoparticles: new advances in breast cancer therapy. *Anti-Cancer Agents Med Chem*. 2012;12(9):1058–1070.
56. Cabeza L, Ortiz R, Arias JL, et al. Enhanced antitumor activity of doxorubicin in breast cancer through the use of poly(butylcyanoacrylate) nanoparticles. *Int J Nanomedicine*. 2015;10:1291–1306. doi:10.2147/IJN.S74378